Electronic Supplementary Material (ESI) for Physical Chemistry Chemical Physics.
This journal is © the Owner Societies 2024

Supplementary information (SI) for

First-principles prediction of ferroelectric Janus Si_2XY (X/Y = S/Se/Te, X ≠ Y) monolayer with negative Poisson Ratios

Yunlai Zhu [a], Zihan Qu [a], Jishun Zhang [a], Xiaoteng Wang [a], Shuo Jiang [a], Zuyu Xu [a], Fei Yang [a], Zuheng Wu [a]*, and Yuehua Dai [a]*

[a] School of Integrated Circuits, Anhui University, Hefei, Anhui, 230601, China.

Corresponding Authors

*E-mail: wuzuheng@ahu.edu.cn (Z.-H. Wu), daiyuehua2013@163.com (Y.-H. Dai)

Table 1. Calculated in-plane elastic constants C_{ij} (N m^{-1}) of Si_2SSe, Si_2STe and Si_2SeTe monolayer.

	C_{11}	C_{12}	C_{22}	C_{66}
Si_2SSe	89.753	-7.361	60.272	8.741
Si_2STe	76.360	-4.569	68.590	7.916
Si_2SeTe	67.235	-5.612	68.397	6.641

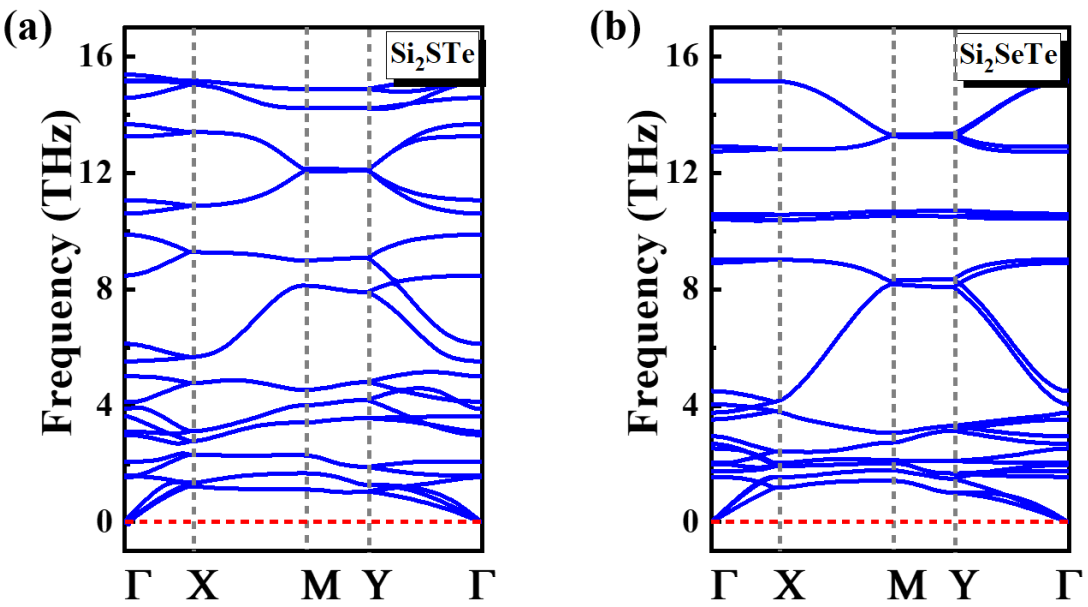

Fig.S1 Phonon dispersion of (a) Si_2STe and (b) Si_2SeTe monolayer, respectively.

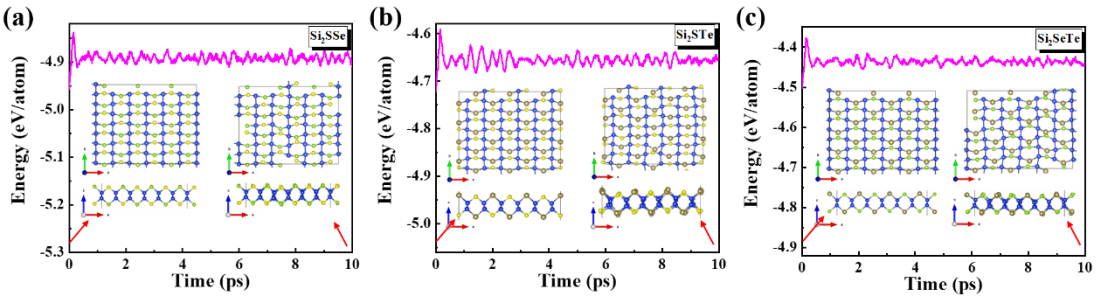

Fig.S2 Total potential energy fluctuation and snapshots of atomic structure of (a) Si_2SSe, (b) Si_2STe and (c) Si_2SeTe monolayer at a temperature of 500 K from AIMD simulation under 0 ps and 10 ps.

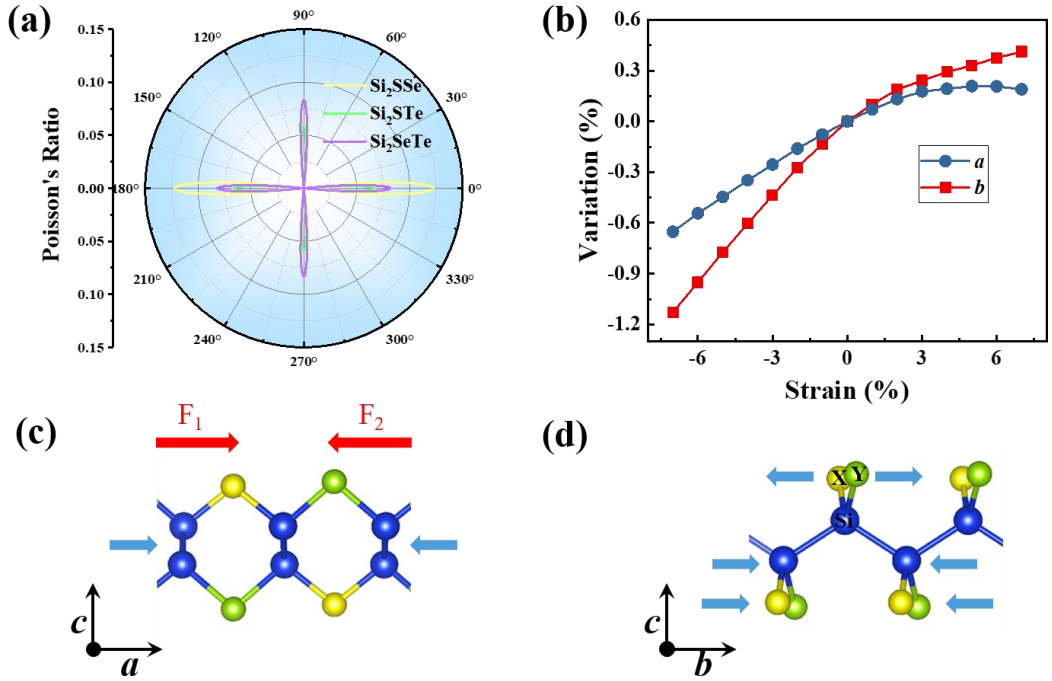

Fig.S3 (a) The NPR of Janus Si_2XY monolayer as a function of the in-plane angle θ. The blue, pink and purple line represent Si_2SSe, Si_2STe and Si_2SeTe, respectively. (b) The strain-variation curve about the strain on *a*-axis with respect to the *b* direction. The evolution of local structures of the Janus Si_2XY monolayer in the *a*–*c* (c) and *b*–*c* (d) planes under uniaxial compression strain.

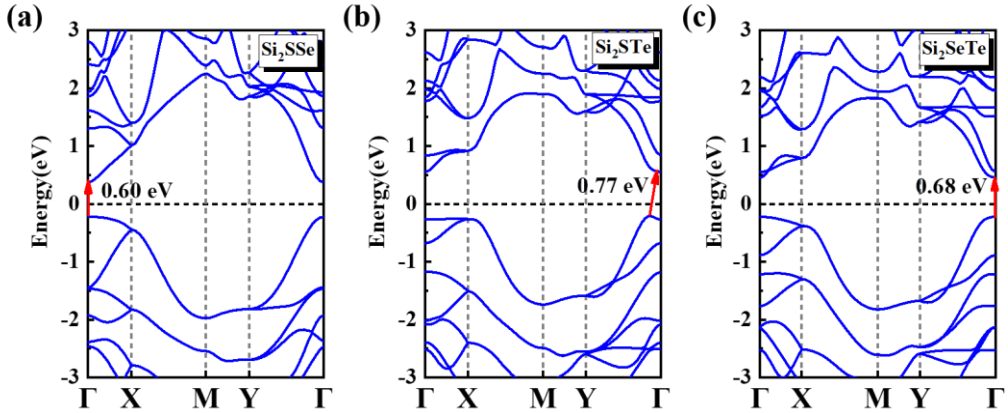

Fig.S4 Electronic band structures of (a) Si_2SSe, (b) Si_2STe and (c) Si_2SeTe monolayer with PBE calculation, respectively.

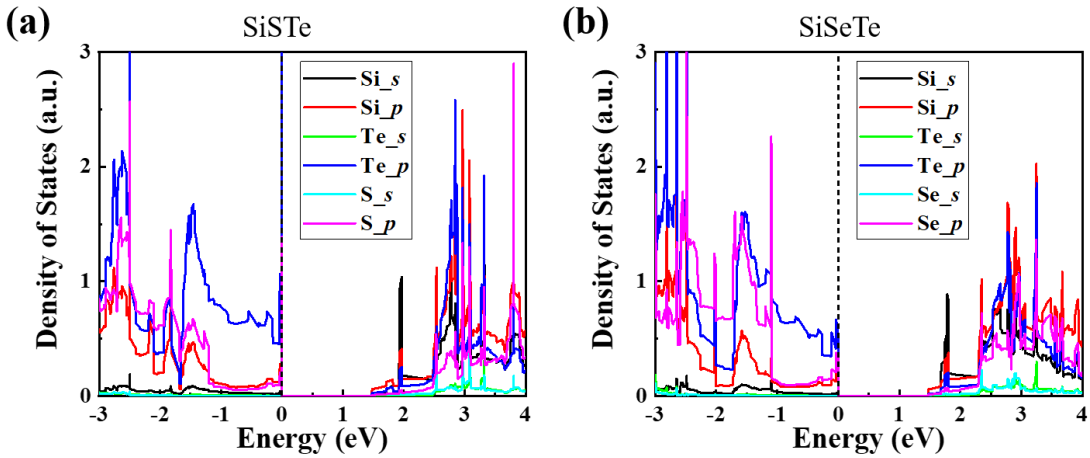

Fig.S5 The corresponding partial density of state (PDOS) of (a) Si_2STe and (b) Si_2SeTe monolayer, respectively.

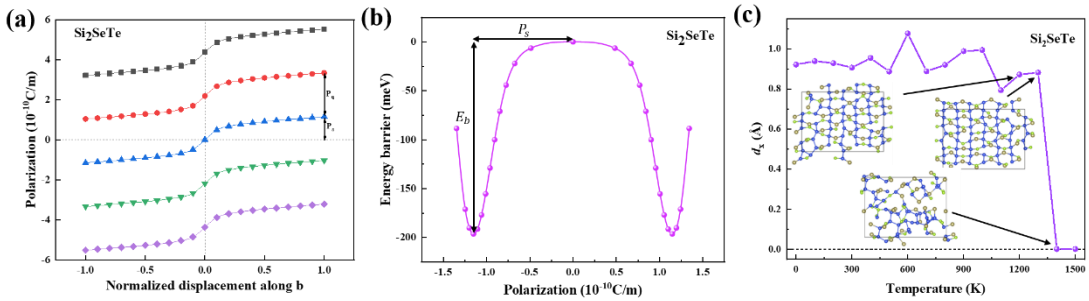

Fig.S6 (a) Polarization P of monolayer Si_2SeTe as a function of normalized displacement along the *b*-axis. P_s and P_q represent the spontaneous and quanta polarization, respectively. (b) Energy curve with the P_s of Si_2SeTe. Phase transition barrier E_b and P_s are marked. (c) Temperature dependence of the average relative displacement between ions in Si_2SeTe using MD simulations. The final atomic structures of Si_2SeTe near the phase transition temperature are depicted.

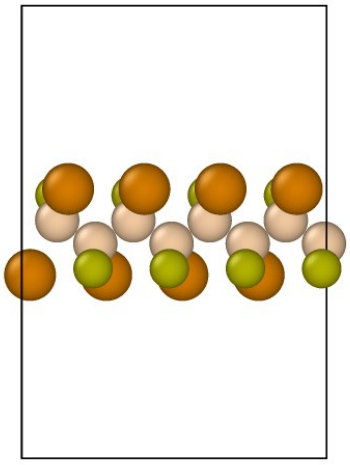

Fig.S7 The AIMD simulations of Si_2STe monolayer with the time step of 4 ps at the temperature of 1200 K. The white, green and orange balls denote Si, S and Te atoms, respectively.

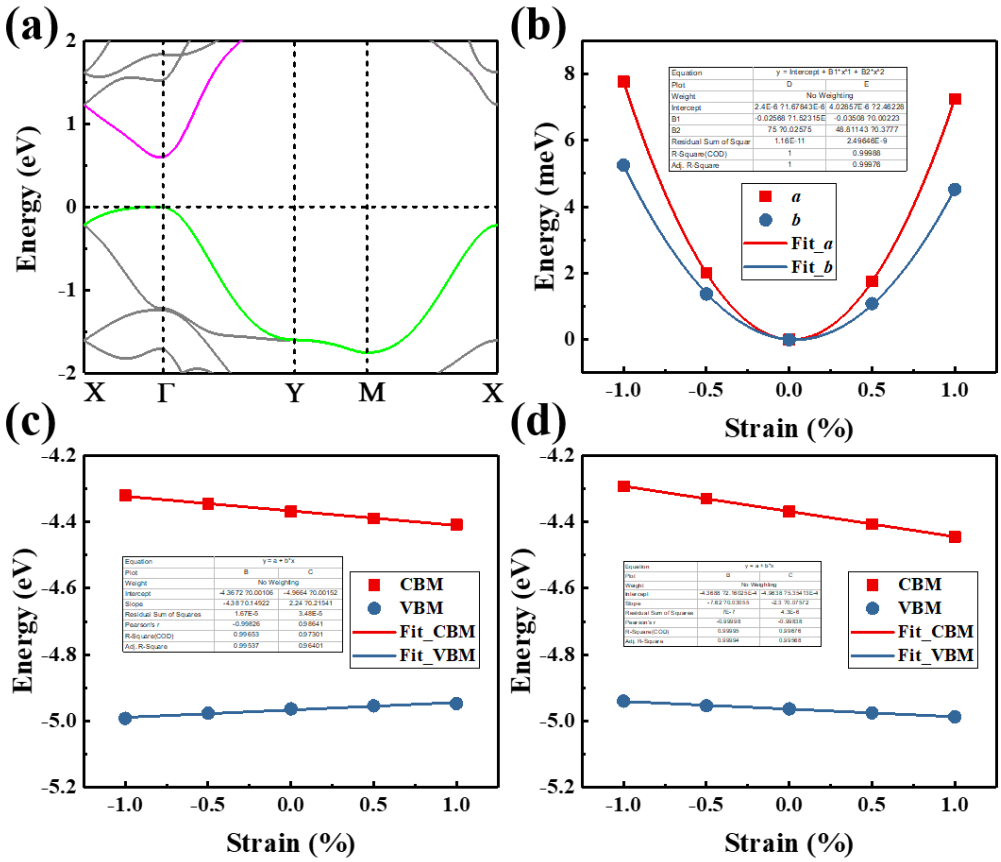

Fig.S8 (a) Electronic band structure of monolayer Si_2SSe with PBE method. (b) The energy shifting and band-edge positions as a function of the (c) *a*-axis and *b*-axis strain along two transport directions of Si_2SSe monolayers. The solid lines indicate the fitting curves.

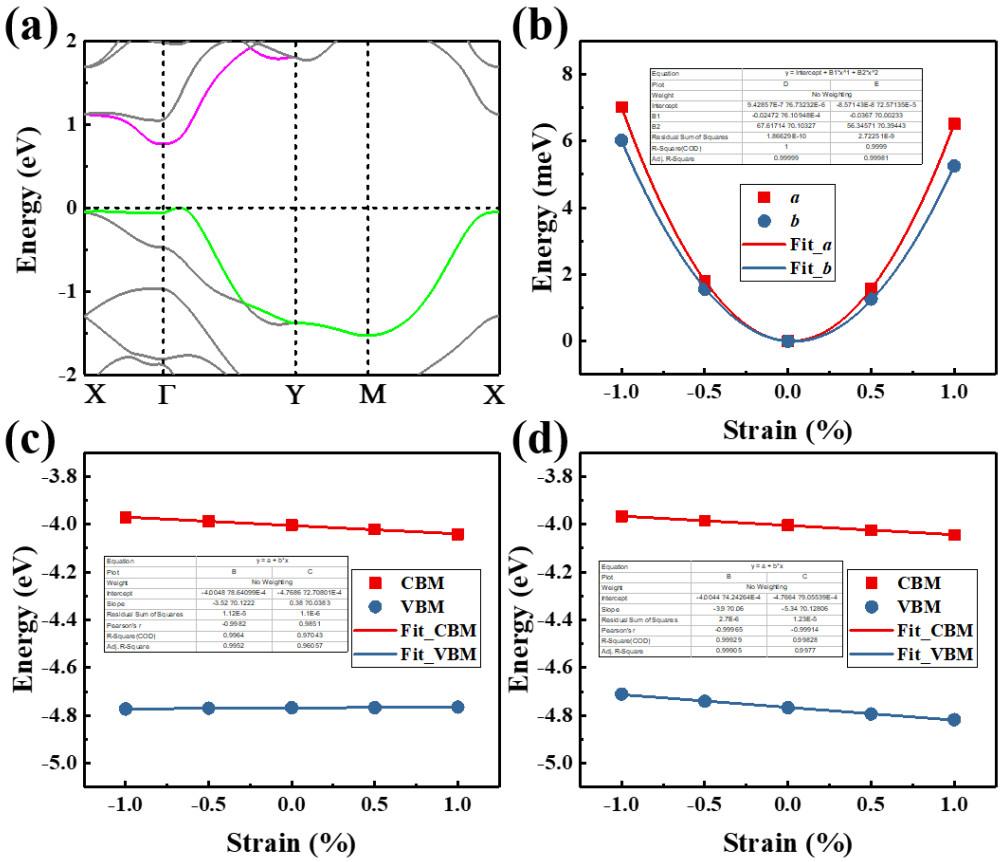

Fig.S9 (a) Electronic band structure of monolayer Si_2STe with PBE method. (b) The energy shifting and band-edge positions as a function of the (c) *a*-axis and *b*-axis strain along two transport directions of Si_2TSe monolayers. The solid lines indicate the fitting curves.

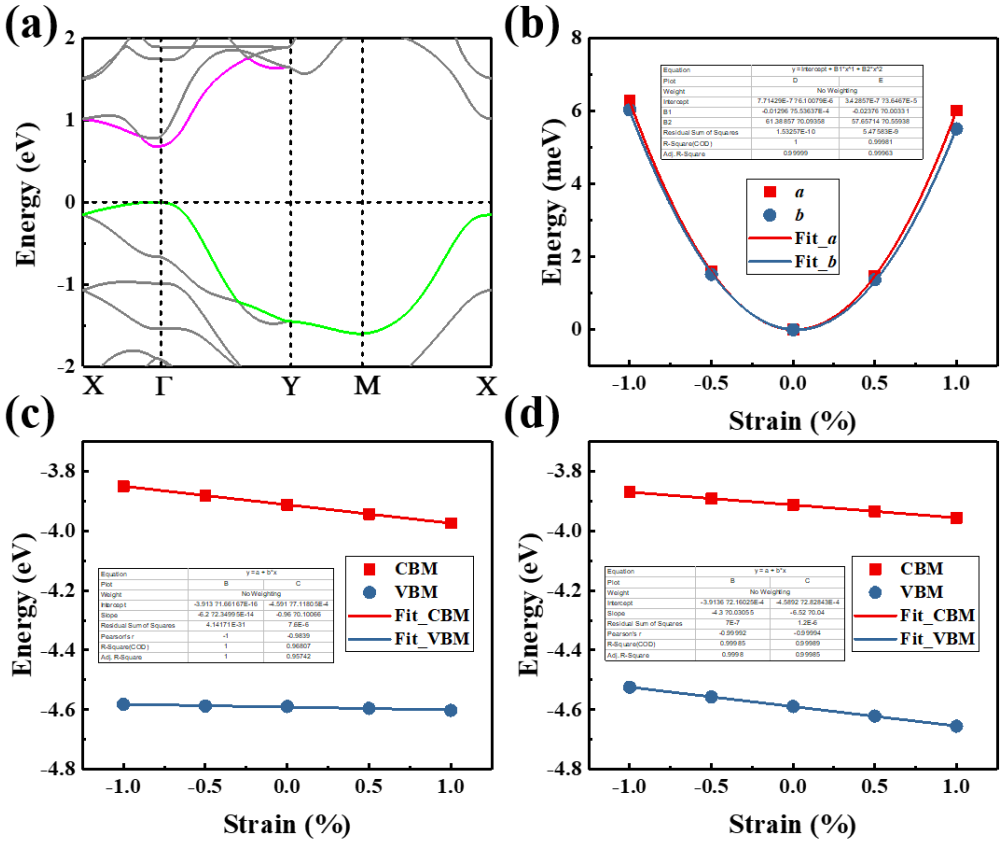

Fig.S10 (a) Electronic band structure of monolayer Si_2SeTe with PBE method. (b) The energy shifting and band-edge positions as a function of the (c) *a*-axis and *b*-axis strain along two transport directions of Si_2SeTe monolayers. The solid lines indicate the fitting curves.